Experimental and Modelling Comparison of the Effects of UV Energy on Liquefaction Efficiency in Coal Liquefaction Mechanism

Yelda ALTINSOY[1*] (iD), Emir H. ŞİMŞEK[1] (iD)

[1]Ankara University, Department of Chemical Engineering

Keywords	Abstract
Liquefaction Kinetic Model Coal MatLab	Coal liquefaction process gives very efficient results, especially for value-added chemicals production from low-quality coal. However, when the literature is examined, notably there is not enough scientific study for liquefaction mechanisms. Here, in this study, There are five different liquefaction mechanisms of Beypazarı coals. It includes four different UV light power and a catalyst environment using 180 watts of UV power. Created first-order linear discrete models were proposed and compared with the experimental results. Additionally, the reaction rate constants for each proposed kinetic model were calculated using the Kalman filter method. However, to evaluate the compatibility of the experimental results and the modeling results, the sum of the squared differences of the values calculated from the experimental data and the models was examined. Because of these studies, it has been observed that the rate constants of direct oil formation from coal at 120 and 180 watts of UV power are at least three times greater than the rate constants for the formation of asphaltene and pre-asphaltene from coal. Simultaneously, The results demonstrate that models with reversible and parallel steps are more compatible with experimental data. Experimental data and modeling results are much more compatible with the studies conducted on Beypazarı coals in a 180-watt UV-catalyzed environment compared to a 180-watt catalyst-free environment. In the presence of ZnO catalyst, the rate constants occurring in the conversion reaction from coal to oil were again three times faster than the conversion rate constants from coal to asphaltene and from coal to preasphaltene. In the modeling and experimental results conducted in the catalyst environment, the efficiency was higher than the catalyst-free environment. The best fit was obtained using model that has both reversible (between asphaltene: coal, asphaltene: oil, and asphaltene: preasphaltene) and irreversible (coal: oil, coal: preasphaltene and preasphaltene: oil) reaction steps. The model also evidenced that reversible reactions are critical on the liquefaction of Beypazarı coal.

1. INTRODUCTION

Coal liquefaction is an advantageous process in which coal can be converted into more valuable and cleaner liquid hydrocarbons that can be used in liquid fuels and petro-chemistry (Cunliffe, 2001; Wang et al., 2009; Li et al., 2017; Gao et al., 2018; Hao et al., 2017; Liu et al., 2018). The main purpose in coal liquefaction processes is to obtain products from coal, primarily petroleum, liquid, asphaltene and pre-asphalten. The main approaches used to convert coal into liquid hydrocarbons revolve around breaking down large, complex "structures" by hydrogenation reactions and increasing the solubility of the organic fraction (Speight, 2008; Li et al., 2017; Gao et al., 2018; Hao et al., 2018). For this purpose, there are two basic liquefaction processes in liquefaction processes. One of them is indirect liquefaction and the other is direct liquefaction. The conversion of the syngas (CO+H$_2$) obtained because of the gasification process of coal into liquid products using special catalysts is known as the indirect liquefaction process of coal (Karacan, 2004). The basis of the direct coal

*Corresponding Author, e-mail: yeldaaltinsoy@enerji.gov.tr

liquefaction process is due to the thermal decomposition of coal in an H-donating solvent using a heat source and hydrogenation of its decomposition products. The solvent used in the process to directly obtain hydrogen gives hydrogen directly in the stabilization of free radicals and provides hydrogen transfer from the hydrogen-rich parts of the coal to other reactive regions that need hydrogen. The resulting reactions provide coal, gas, liquid and solid products (Allen & Gavalas, 1984; Hsiang-Hui & Stock, 1984).

The coal liquefaction process, which occurs in a hydrogen donor environment, depends on many independent chemical reactions. These reactions support the formation of many active and inactive substances as they progress. Stabilization of active species and free radicals is of great importance in terms of ensuring reaction efficiency (Cronauer at al., 1979; Mohan & Silla, 1981; Huang et al., 1998; Li et al., 2008; Şimşek et al., 2017). For this reason, to understand these reactions and mechanisms, the direction of studies recently has been directed to this area (Farcasiu et al., 1977; Cronauer et al., 1978; Han et al., 1978; Shah et al., 1978; Shalabi et al., 1979; Angelova et al., 1989; Ceylan & Olcay, 1998; Şimşek et al., 2017). Liebenberg & Potgieter (1973) proposed liquefaction mechanism includes following steps asphaltene from coal and heavy oil formation from asphaltene, as well as two parallel reactions; coal → asphaltenes and coal → heavy oil reactions. Cronauer et al. (1978) conducted a study on the lower bituminous coal conducting in a continuous stirred reactor (CSTR) with the help of anthracene oil and phenanthrene solvents, and a first-order irreversible kinetic analysis of coal → oil, oil → asphaltene, coal → preasphaltene, preasphaltene → asphaltene, coal → asphaltene and coal → gas. model has been proposed. The kinetic mechanisms of dissolution in the presence of tetralin in a bituminous coal with high volatility were investigated and three model mechanisms were proposed by Ayappa et al. (1991). Two models were predicted for the liquefaction kinetics of the coals dissolving in the presence of tetralin. A model is the same as the one proposed by Shalabi et al. (1979).

Significant liquefaction reactions occur when coals are exposed to direct heat with the use of a thermal source in pressurized furnaces due to long heating and cooling periods. However, it does not show realistic liquefaction reaction mechanisms under these reaction conditions with the use of a pressure furnace and thermal source. Therefore, in the direct liquefaction process of coal, the use of microwave or UV light sources, which increases efficiency due to short startup and internal heating periods, becomes more effective as a heat source (Ayappa et al., 1991).

In both two studies, the liquefaction mechanisms of coal in the presence of tetralin and the formation rate constants of preasphalten, asphaltene and oil were investigated using microwave source (Şimşek et al., 2001; Shui et al., 2010).

The rate of formation of preasphaltene, asphaltene and oil was investigated during the liquefaction of six different reactive coals in tetralin as a hydrogen donor solvent using microwave heating in the literature (Şimşek et al., 2001; Shui et al., 2010). Within the scope of the studies, five different liquefaction models were determined and it was assumed that the reactions occurring here were irreversible and pseudo-first order. It has been observed that the reactions proceed in parallel in the conversion mechanism from coal to asphaltene, pre-asphaltene and oils. It is noteworthy that coal has much higher carbon content in parallel reactions. Five different liquefaction models, defined as irreversible and pseudo-first order, were proposed and studied. Models consisting of parallel liquefaction from coal to preasphaltenes, asphaltenes and oils show that coal with higher carbon is most appropriate, while models involving serial and parallel liquefaction reactions show that lower carbon coals are more suitable.

Two of the studies conducted with the use of UV rays in the liquefaction of coal is the studies by Yürüm and Yiğinsu (1982) and Söğüt and Olcay (1998). In these studies, photochemical reactions of coal were investigated without the need for high pressure and temperature. It has been determined that oil formation in liquid products formed because of photochemical reactions has much higher formation rates than asphaltene and preasphalten formations. Therefore, the use of UV rays in coal liquefaction processes has made it more effective (Yürüm & Yiğinsu, 1982; Söğüt & Olcay, 1998). In a study by Doetschman et al. (1992) the liquefaction of coal in a tetrahydrofuran solvent with the effect of UV rays was investigated in the coal liquefaction process. In this study, different coal samples were irradiated at different powers and showed that the effect of UV irradiation power was directly proportional to the liquefaction efficiency. The study proved that liquefaction is five times more efficient in coal exposed to continuous irradiation compared to the

liquefaction process performed in the dark without the use of UV irradiation power. Studies have shown that the stimulation of molecules in the solvent/coal extract using UV causes the fragmentation of coal particles. When the extract structures were examined, it was seen that the fragmentation caused by the UV rays in the coal macromolecular structure chain provided the return to the aromatic structure (Doetschman et al., 1992).

2. EXPERIMENTAL STUDIES

This study constitutes the kinetic modeling of the coal liquefaction prosses. In order to determine the kinetic mechanism, the MatLab programme was performed with experimental results. For a highly efficient determination of kinetic model study, it is necessary to find out the kinetic approach that is compatible with the experimental results.

2.1. Experimental Data

The experimental data used in the discrete-time models of coal liquefaction models in this study were obtained from the study by Karacan (2004). Coal samples were supplied from Beypazarı-Çayırhan and were crushed and then ground in size using a mill-ball. The grinded samples were sieved with a particle size of sub-300 microns using standard lab scale sieves. The coal samples were then dried under atmospheric conditions until they reached a constant weight and then stored in plastic bottles with lids to be used in the experiments. Experiments were conducted with different UV light powers of 0, 60, 120, and 180 Watt using a tetralin/charcoal mixture of 5/1 by weight for 1, 2, 3, 5, and 10 days.

To investigate the effect of UV power in liquefaction experiments, a UV chamber whose energy power changes approximately 30 to 210W was used. In this chamber, a round bottomed flask with a volume of 500 ml and a magnetic stirrer with adjustable stirring speed was used. For the non-catalytic study, 15 g coal and 75 g of tetralin were weighed into the quartz flask, and for catalytic tests, 0.75 g catalyst was added to the quartz flask at a ratio of 5% catalyst/lignite by weight. However, in the catalyst addition stage, TiO_2 and ZnO were added to the medium by physical mixing, while ZnO was added by being absorbed into the coal particles. The addition of tetralin was added after the homogenization of the charcoal catalyst mixture had taken place before the experiment under catalytic conditions.

Before UV experiments to be conducted in both catalytic and non-catalytic conditions, the mixtures were mixed for 2-3 minutes in order to increase the interaction of the particles with each other during the reaction. After the experimental conditions were established, the desired UV rays were exposed to the tetralin/catalyst/coal and tetralin/coal mixtures in the round bottomed flask and the reactions were conducted. However, experiments with a power of 0 watts were conducted in a dark environment. All experiments were conducted at atmospheric pressure and room temperature, at the end of the determined test times, the system was turned off and the reaction temperatures were physically measured. After it was defined that the measured reaction temperatures did not exceed 33 °C, the round bottomed flask in the UV chamber was removed and the mixture was filtered and the solid/liquid phases were separated from each other. The remaining fractions in the flask were obtained by washing with tetrahydrofuran and the solid phase was first washed with this mixture and then washed again with tetrahydrofuran. The filtrate obtained from the washed solid phase was mixed with the liquid phase. Before mixing, rotay evaporator removed THF under atmospheric pressure. As a result, the liquid phase contains tetralin and charcoal dissolved in tetralin.

To keep the tetralin in a certain amount, it was ensured that the tetralin was removed from the mixture under vacuum and the concentration was increased in the rotary evaporator. To allow the liquid product to be separated into fractions as oil, asphaltene and preasphalten, the concentrated mixture was kept overnight by adding 200 ml hexane. An overnight waiting period facilitated the separation of the oils from the asphaltene and pre-asphaltene, as it caused the oils to dissolve in hexane. The removal of hexane from the filtrate was achieved using a rotary evaporator and oils were obtained. Due to the dissolution of asphaltenes in toluene, 200 ml toluene was used to separate the remaining mixture from the preasphalten, and toluene was also removed in the rotary evaporator. Products insoluble in toluene were taken from the mixture as preasphalten. In this way, oil, asphaltene and preasphaltene formations obtained from coal liquefaction process were determined. Experimental studies are given in Table 1 by calculating the percentage of products (oil, asphaltene and preasphalten) obtained at each UV exposure for different time periods and the weight percentage of

liquefied products (preasphaltenes, asphaltenes and oils) per weight of lignite (daf) used. Additionally, the physical properties of coal are given in Table 2.

Table 1. *Beypazarı coal experimental study (Karacan, 2004)*

UV Power	Time (day)	Oil %	Asphaltene %	Preasphaltene %	Liquid product %
0 W (in dark)	1	4.81	0.46	1.03	6.30
	2	4.34	0.75	0.97	6.06
	3	4.10	0.88	0.87	5.85
	5	4.48	0.91	0.54	5.93
	10	5.04	1.20	0.57	6.81
60 W	1	13.53	1.88	0.38	15.79
	2	15.98	2.77	1.10	19.85
	3	15.36	2.91	0.61	18.88
	5	15.47	2.80	0.48	18.75
	10	13.60	6.26	1.26	21.12
120 W	1	13.58	2.33	0.40	16.31
	2	15.75	3.82	0.80	20.37
	3	14.41	3.25	1.16	18.82
	5	17.03	2.05	1.87	20.95
	10	20.91	3.82	2.01	26.74
180 W	1	13.49	3.10	0.80	17.39
	2	18.36	1.81	0.40	20.57
	3	17.72	2.38	1.14	21.24
	5	19.23	2.09	0.42	21.74
	10	27.53	2.70	2.76	32.99
180 W TiO$_2$	1	17.36	2.38	0.64	20.38
	2	15.16	2.66	0.68	18.50
	3	19.92	2.20	1.01	23.13
	5	15.78	1.11	0.52	17.41
	10	24.17	3.15	2.67	29.99
180 W ZnCl$_2$	1	13.37	1.76	0.86	15.99
	2	15.92	3.52	1.08	20.52
	3	14.65	2.31	1.31	18.27
	5	28.99	2.84	1.42	33.25
	10	16.67	2.71	0.96	20.34
180 W ZnO	1	12.15	1.46	0.26	13.87
	2	14.52	2.83	0.37	17.72
	3	16.71	2.91	2.01	21.63
	5	23.78	1.27	0.26	25.31
	10	26.12	1.50	0.36	27.98

Table 2. *Analysis of Beypazarı coal samples (Karacan, 2004)*

Ultimate Analysis (w/w %)	
Moisture	13.00
Ash	25.55
Volatile Matter	29.19
Fix Carbon	32.26

Sulfur Distribution Hit (w/w %)	
S_{total}	4.59
S_{oxy}	3.52

Elemental Analysis (w/w %)	
C	69.56
H	4.50
N	1.25
S_{oxy}	4.72
O	19.97

Maseral Composition (vol %)	
Huminite	94.3
Liptinit	2.60
Inertinite	3.10

Lower Calorific Value (kcal/kg)	3978

2.2. Recommended Coal Liquefaction Models

In the model suggested for five different coal liquefaction depending on three parameters; (A) represents the reactive coal, (B) the asphaltene liquefied from the reactive coal, (C) the preasphaltenes and (D) the oils. In the literature, many reaction models have been investigated for the liquefaction mechanism in coals of different structures. In this study, five different models proposed for Beypazarı coals are given in Figure 1. The models consist of parallel and series as well as reversible and irreversible steps. The gaseous products were not obtained due to the low reaction (at 25°C) temperatures, and in this case, possible reaction steps were removed from the proposed models. The reaction rate equations of the proposed models are given in Equations 1-20. In this study, the comparison of experimental data with modeling data is also evaluated. The mechanisms given in Model 1 and Model 2 were explained as suggested by Shalabi et al. (1978). In Model 1, there is a transformation from coal to preasphalten, from preasphalten to both asphaltene and oils due to serial reactions, while oil is formed from asphaltene at the same time. All reactions are assumed to occur first-order and irreversibly. In Model 2, while direct oil conversion occurs from coal, there are also direct asphaltene and pre-asphaltene formations from coal, and asphaltene and oil formations from pre-asphaltene formed from coal. In this model, the reactions are considered parallel, first-order and irreversible. In a study proposed by Şimşek et al. (2021) Model 3 includes reversible, irreversible parallel and serial first-order reactions. This model, which includes reversible and irreversible mechanisms, which is one of the remarkable details in the explanation of the coal liquefaction mechanism, is discussed again in this study. Model 3, in addition to Model 2, consists of reversible reaction steps between coal ↔ asphaltenes, asphaltenes ↔ preasphaltenes and asphaltenes ↔ oils. Model 4 and Model 5 are the models recommended within the scope of this study, and Şimşek (1997) and Söğüt (1997) in both models are the models recommended after a decrease in oil yield after a maximum when their studies are examined. Therefore, Models 4 and 5 are assumed to have steps in which oil gives reversible reactions. Model 4 assumes the reversible formation of oils and preasphaltenes, preasphaltenes, oils from coal, as well as the formation of asphaltenes, asphaltenes, preasphalthenes and oils from coal. In Model 5, reversible formation of asphaltenes and oils from coal and reversible formations of oils from preasphaltenes and asphaltenes are predicted.
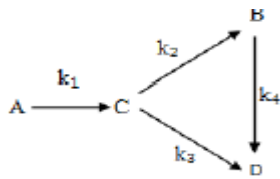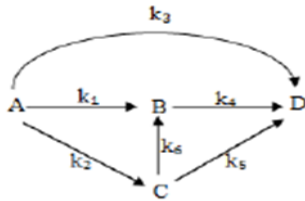
$$\frac{dA}{dt} = -k_1 A \tag{1}$$

$$\frac{dB}{dt} = k_2 C - k_4 B \tag{2}$$

$$\frac{dC}{dt} = k_1 A - (k_2 + k_3)C \tag{3}$$
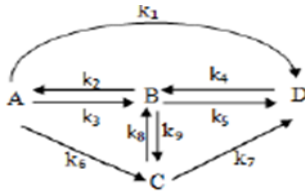
$$\frac{dD}{dt} = k_3 C + k_4 B \tag{4}$$

$$\frac{dA}{dt} = -\theta A \tag{5}$$

$$\frac{dB}{dt} = k_1 A + k_6 C - k_4 B \tag{6}$$

$$\frac{dC}{dt} = k_2 A - (k_5 + k_6)C \tag{7}$$
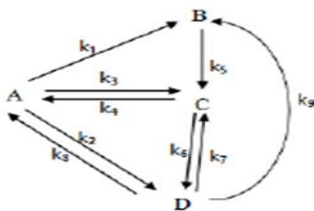
$$\frac{dD}{dt} = k_3 A + k_4 B + k_5 C \tag{8}$$

$$\frac{dA}{dt} = k_2 B - (k_1 + k_3 + k_6)A \tag{9}$$

$$\frac{dB}{dt} = k_4 D + k_8 C + k_3 A - (k_2 + k_5 + k_9)B \tag{10}$$

$$\frac{dC}{dt} = k_6 A + k_9 B - (k_7 + k_8)C \tag{11}$$

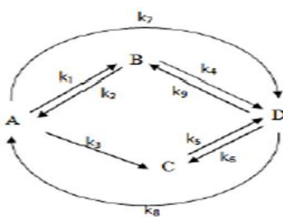$$\frac{dD}{dt} = k_1 A + k_5 B + k_7 C - k_4 D \tag{12}$$

$$\frac{dA}{dt} = k_4 C + k_8 D - (k_1 + k_2 + k_3)A \tag{13}$$

$$\frac{dB}{dt} = k_1 A + k_9 D - k_5 B \tag{14}$$

$$\frac{dC}{dt} = k_3 A + k_5 B + k_7 D - (k_4 + k_6)C \tag{15}$$

$$\frac{dD}{dt} = k_2 A + k_6 C - (k_7 + k_8 + k_9)D \tag{16}$$

$$\frac{dA}{dt} = k_2 B + k_8 D - k_7 A \tag{17}$$

$$\frac{dB}{dt} = k_1 A + k_9 D - (k_2 + k_4)B \tag{18}$$

$$\frac{dC}{dt} = k_3 A + k_6 D - k_5 C \tag{19}$$

$$\frac{dD}{dt} = k_7 A + k_4 B + k_5 C - (k_6 + k_8 + k_9)D \tag{20}$$

Figure 1. *Suggested coal liquefaction models;* ***A)*** *Reactive coal,* ***B)*** *Asphaltene,* ***C)*** *Preasphaltene,* ***D)*** *Oil*

2.3. Comparison of Models with Experimental Data

The compatibility of the proposed liquefaction reactions with the experimental results regarding the liquefaction mechanisms of coal belonging to the Beypazarı region has been revealed by creating first-order discrete-time models. The Kalman Filtering method was used for each reaction rate constant in the models and was determined using the MatLab program (version 7.11). If given as an example; The discrete-time model used for Model 2

Additionally, the reaction rate constants for each reaction in the models are determined using a MatLab program (written in ver 7.11, The MathWorks Inc. Natick, MA, USA) using the Kalman filter. For example, discrete-time model equations used for Model-1 in this study are given in Equations 21-24.

$$C_A (i+1) = CA_i (1 − (k_1 + k_2 + k_3) \Delta t) \tag{21}$$

$$C_B (i+1) = CB_i (1 − k_4 \Delta t) + (k_1 CA + k_6 CC_i) \Delta t \tag{22}$$

$$C_C (i+1) = CC_i (1 − (k_5 + k_6) \Delta t) + k_2 CA_i \Delta t \tag{23}$$

$$C_D (i+1) = CD_i + k_3 CA_i \Delta t + k_4 CB_i \Delta t + k_5 CC_i \Delta t \tag{24}$$

Where, C_A is unreacted coal (daf) and C_B, C_C, C_D are percentages of asphaltene, preasphaltene and oil yield, respectively.

In the literature, the Kalman filter method is an algorithm in which a set of measurements observed over time can be used, including statistical noise and other errors. It can predict unknown variables more precisely than those based on a single measure (Wei et al., 2013). To control a dynamic system, it is necessary to know what is happening in the system. However, it is impossible to identify every variable in an impossible process, especially for measuring liquefaction such as coal processes. Therefore, the Kalman filter can predict state variables from available known data with minimal change to unknown current data. The rate constants of the proposed liquefaction mechanisms can be estimated using the Kalman filter, and there are many studies in the literature with the use of MatLab (Grewal & Andrews, 2001; Welch & Bishop, 2006; Şimşek et al., 2017; 2019).

3. CONCLUSIONS AND DISCUSSIONS

The use of first-order linear discrete-time models for the compatibility of experimental data and data obtained from models is a study in the literature. Simultaneously, a program was created in the MatLab application to calculate the rate constants of the reactions occurring, and predictions were made with the Kalman Filtering Method (Kalman, 1960). Within the scope of this study, the experimental data and the most compatible model of the proposed model are given in Model 3 and Equation 25. The compatibility of this model with the experimental data was decided by looking at the square of the difference between the data calculated from the model and the experimental data (Kavuştu, 2012).

$$\sum_i (y_{m_i} − y_{e_i})^2 = (AS_m − AS_e)^2 + (PAS_m − PAS_e)^2 + (YA_m − YA_e)^2 \tag{25}$$

Here;

y_{m_i} and y_{e_i}	= Values calculated from the model and experimental data
AS_m and AS_e	= Asphaltene yields calculated from the model and experimental data
PAS_m and PAS_e	= Preasphaltene yields calculated from the model and experimental data
YA_m and YA_e	= Oil yields calculated from the model and experimental data

When examining the compositional properties of coal to examine their behavior in direct liquefaction, it is impossible to say that a single property sufficiently predicts the transformations for all coal. Therefore, to understand the liquefaction behavior of coal, correlations with sulfur, reactive maceral and volatile matter contents, vitrinite reflection and H/C ratios were established for coals from certain geological regions. Based on this study, bituminous coals provide higher conversions than low-grade coals at short residence times, but under typical hydro-liquefaction processing conditions, distillate yields are generally higher than low-grade coals. The lack of information about aromatic, aliphatic and heteroatomic groups and the concentrations of low molecular weight components in coals preclude more precise structural correlations with liquefaction behavior. Analytical results from studies on how organic coal structure affects liquefaction are still being

evaluated. (Snape, 1987). It is assumed that coals provide the formation of coal liquefaction patterns due to their amorphous, cross-linked polymeric structure. Aromatic structures with high molecular weight in coal containing heteroatomic structure form the macromolecular structure of these coals and this structure supports the formation of many free radicals due to its easy exposure to photochemical decomposition. Free radicals can easily react with hydrogen or polymerize with other molecules. Here, the hydrogen donor source is tetralin, the hydrogen donor solvent. Low molecular weight and hydrogen-rich products, namely, oils, which are formed because of the stabilization of free radicals with hydrogen, can be produced very easily. In contrast, the formation of high molecular weight H/Cs can be observed due to the polymerization of free radicals without reversible and irreversible reactions. In Table 3, the squares of the difference between Model 1 and experimental data and the rate constants formed at different UV light powers are given.

Table 3. *The squares of the difference between Model 1 and the experimental data and the rate constants (h^{-1}) and the percent liquid yields at different UV powers*

UV Power (W)	$\sum_i (y_{m_i} - y_{e_i})^2$	Rate constant (h^{-1}) x 10^3				oil conversion % experimental
		k_1	k_2	k_3	k_4	
0	83.8723	5.5	12.3	13.2	10.2	Day 10 5.04
60	655.9149	14.1	14.1	15.9	10.4	Day 2 15.98
120	740.3083	16.2	13.9	16.9	10.7	Day 10 20.91
180	965.5916	18.0	14.1	18.1	10.8	Day 10 27.53
180/TiO_2	963.1773	16.8	13.9	17.4	10.7	Day 10 24.17
180/$ZnCl_2$	1033	16.8	14.1	17.5	10.7	Day 5 28.99
180/ZnO	926.6212	16.8	13.9	18.0	10.8	Day 10 26.12

In Figure 2, the comparison of the data obtained from Model 1 with the experimental studies conducted at four different powers, 0, 60, 120, and 180 Watt UV power, is given graphically.

In Model 1, it is assumed that there are first-order irreversible reactions from reactive coal to preasphalten, from preasphalten to asphaltene and oils in parallel and from asphaltene to oils. At Figure 2, although the experiments conducted in the dark are more compatible with Model 1, Model 1 is completely incompatible with the experimental data. The assumed approach in this model is that the bonds will break during the coal liquefaction process (Şimşek et al., 2017). In the experiments conducted for the decomposition of coal using UV energy, it is seen that as the UV light power increases, the oil formations and generally increased around the 10th day, but these increases in the model are not at the same rate as the experimental data. In the evaluations for the decomposition of coal under UV light, firstly, polar groups are formed due to decomposition by UV effect, and then pre-cracking products due to liquefaction reaction, which can be considered as pre-asphalten. Preasphaltenes are H/Cs insoluble in toluene. In fact, Arrhenius cracking and coal chemistry do not support such possibilities. Generally, in liquefaction processes, it can be deduced that the weakest bonds on the structure are the bonds that dissociate in liquefaction processes. The weakest bonds can form two products, both of which have the property of dissolving in toluene, and only preasphaltene formations can be seen from the breaking of the less weak bonds. Another assumption considered while creating the model is that H/Cs insoluble in toluene can turn into soluble products in toluene or hexane. Additionally, coal liquefaction processes in the hydrogen donor solvent environment support the formation of free radicals. Hydrogens from solvent (Şimşek et al., 2017) can stabilize free radicals because solvent donates hydrogen under the influence of UV light to the free radicals (Şimşek et al., 2017). Due to this stabilization, products with smaller molecular weights are directly produced (Şimşek et al., 2017).
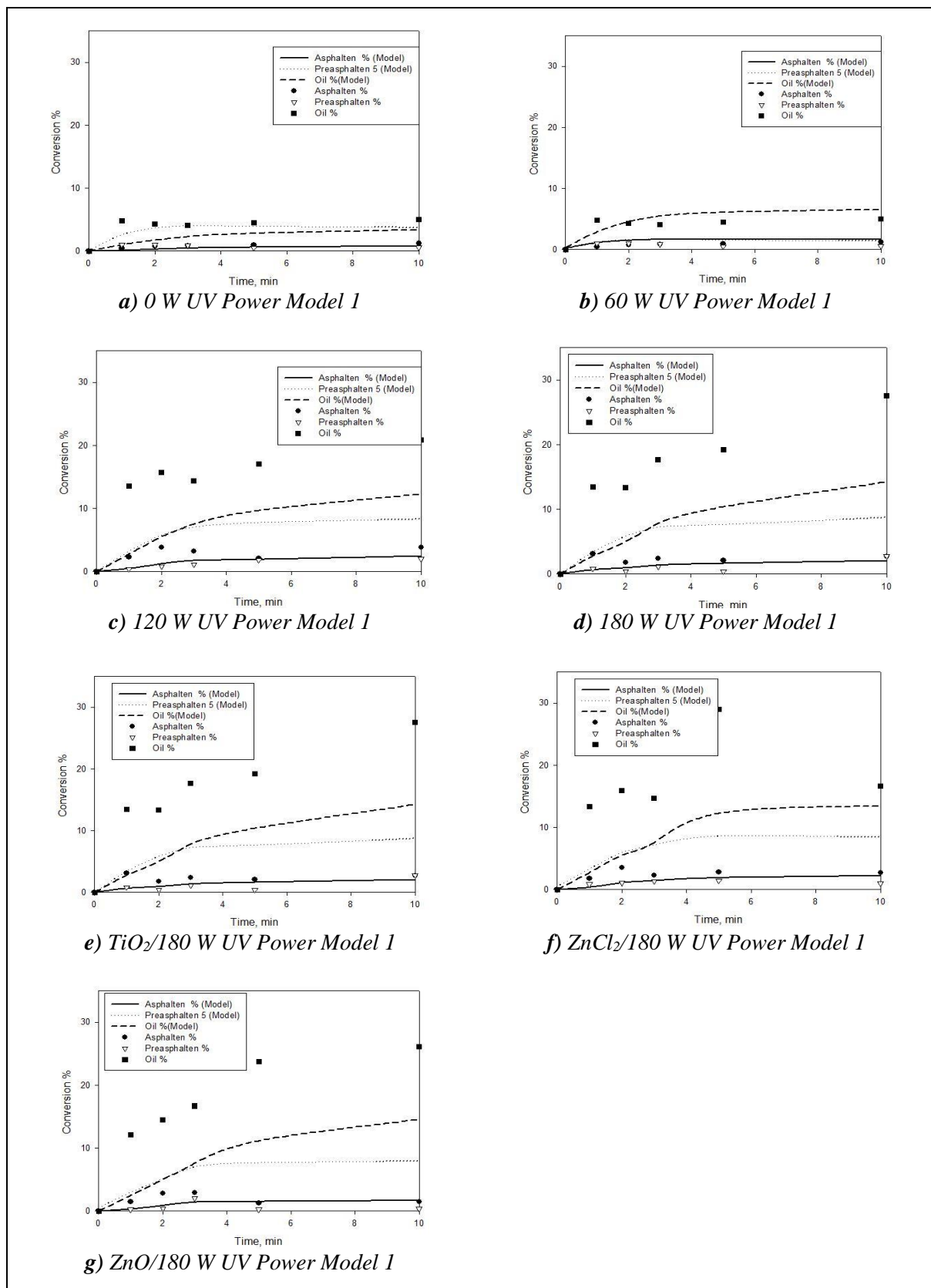
Figure 2. *Comparison of the liquefaction mechanism obtained using Model 1*
with experimental data at different UV powers
a) *0 W,* ***b)*** *60 W,* ***c)*** *120 W,* ***d)*** *180 W* ***e)*** *TiO₂/180 W* ***f)*** *ZnCl₂/180 W* ***g)*** *ZnO/180 W*

The reason for the inconsistency with the experimental data in Model 1 is the properties of coal, other than pre-asphalten, which is formed as insoluble in toluene. Because pre-asphaltene formations are very few both experimentally and modelally under the effect of each UV power. The data obtained from Model 2 and the squares of the experimental data differences and the rate constants formed at different UV light powers are given in Table 4.

In Model 2, asphaltenes (B), preasphaltenes (C) and oils (D) and additionally preasphaltenes (C) oils (D) are formed from coal (A) by parallel reactions, as well as preasphaltenes (C) asphaltenes (B) and oils from asphaltenes (D) formation is assumed. In this model, there are no reversible reactions and all reactions are deemed first order. The square of the differences between the experimental data and the data obtained from the model was the lowest, as in Model 1, in the studies conducted in the dark environment. However, when Model 2 is compared with Model 1, the square of the differences is more consistent than Model 1, but when the graphs given in Figure 3 are examined, the consistency with the experimental data is not better. Notably, asphaltene formations are quite parallel in the data obtained from the model with the experiments conducted in the dark in Model 2, but it is not very consistent for the hexane-soluble oil yields. However, asphaltene and pre-asphaltene formations generally follow a flat course after the 2nd day. In the presence of 180 Watt UV light, oil formations are in full agreement with the experimental data. As a result, it shows that the Model-2 model cannot provide a good definition of the liquefaction of Beypazarı coal for four different UV powers. The inconsistency between Model-2 and experimental data indicates that hexane-soluble H/Cs are more common in the formation of oils, as observed in Model-1.

Table 4. *The data obtained from Model 2 and the squares of the experimental data and the rate constants and the oil formation percentages at different UV light powers*

UV Power (W)	$\sum_i (y_{m_i} - y_{e_i})^2$	Rate constant (h^{-1}) x 10^3						oil conversion % experimental
		k_1	k_2	k_3	k_4	k_5	k_6	
0	50.7958	1.5	1.2	5.5	10.1	-	-	Day 10 5.04
60	252.4420	6.1	3.0	17.5	9.9	10.2	10.0	Day 2 15.98
120	188.4263	5.7	4.1	20.6	10.3	10.2	10.0	Day 10 20.91
180	192.3157	5.4	4.5	24.6	10.7	10.4	10.0	Day 10 27.53
180/ TiO$_2$	316.0903	5.0	4.1	22.9	10.4	10.2	10.0	Day 10 24.17
180/ZnCl$_2$	369.4902	5.4	3.8	22.9	10.4	10.3	10.0	Day 5 28.99
180/ZnO	139.3742	4.6	3.4	24.8	10.7	10.4	10.0	Day 10 26.12

For this reason, it is important to make assumptions on models with reversible reactions to achieve a more realistic model fit. Model 3 assumes reversible and irreversible reactions. The sum of the squares of the difference of the experimental data obtained from model 3, the rate constants and experimental oil conversion rates are given in Table 5.

In Model 3, in addition to the reversible formation of both oil (D) and preasphaltene (C) from coal (A), asphaltene (B) from coal (A), oils (D) from coal (A), pre-asphaltenes (C) and oils (D) from pre-asphaltenes (D) is assumed to be irreversible and first-order formation.
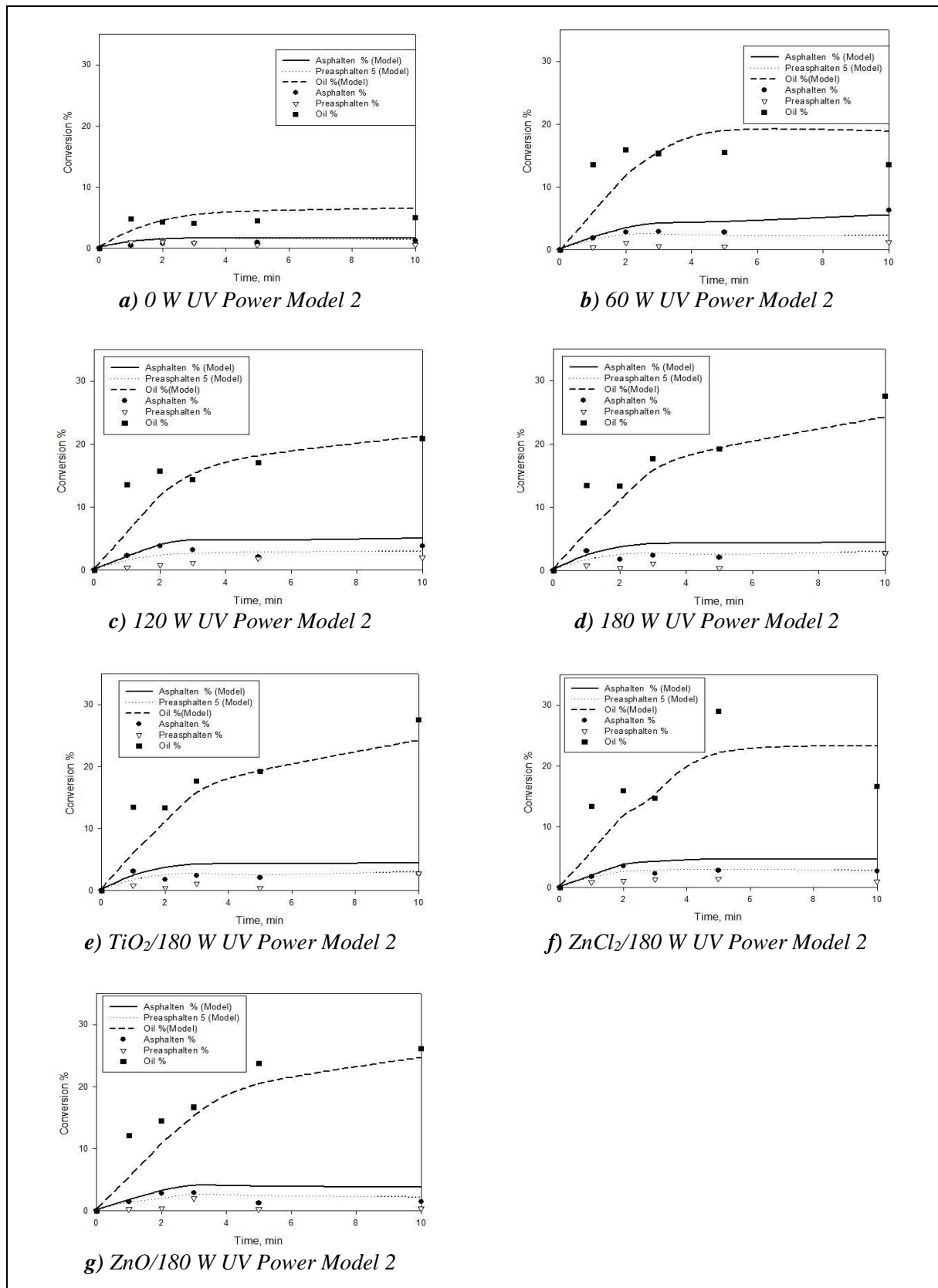
Figure 3. *Comparison of the liquefaction mechanism obtained using Model 2*
with experimental data at different UV powers
a) 0 W, b) 60 W, c) 120 W, d) 180 W e) TiO₂/180 W f) ZnCl₂/180 W g) ZnO/180 W
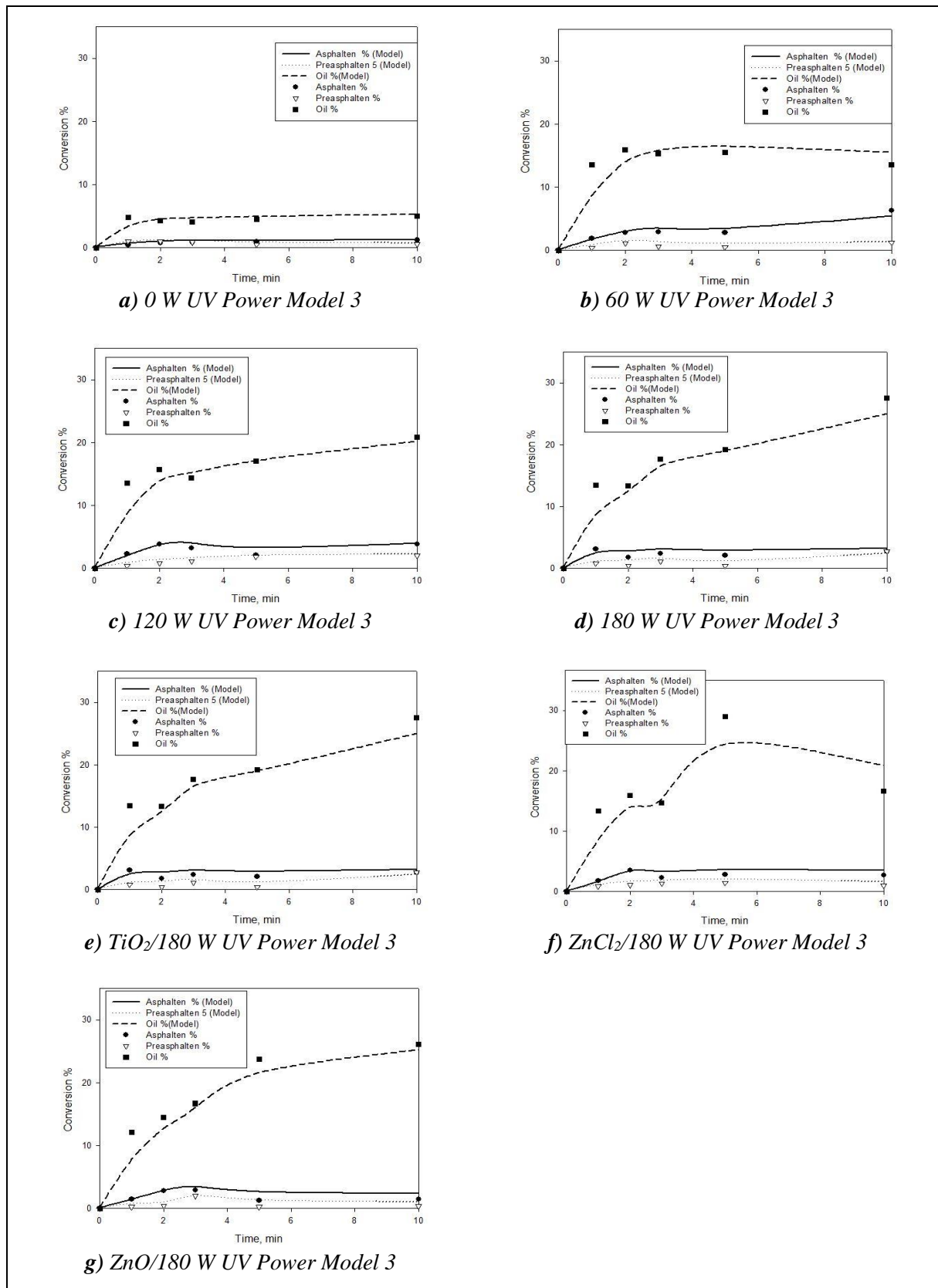
Table 5. *The data obtained from Model 3 and the squares of the experimental data and the rate constants and the oil formation percentages at different UV light powers*

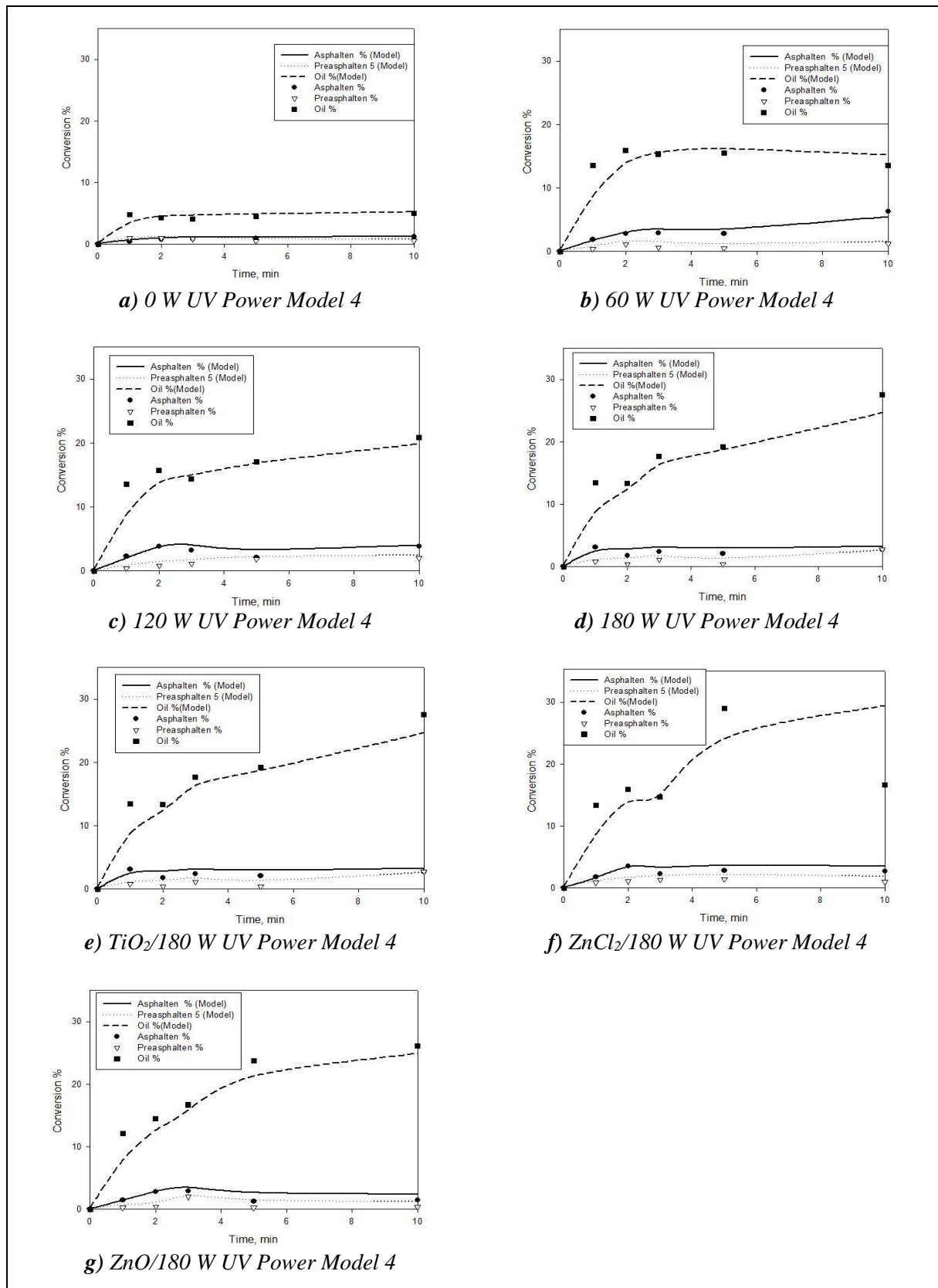| UV Power (W)	$\sum_i (y_{m_i} - y_{e_i})^2$	Rate constant (h⁻¹) x 10³									oil conversion % experimental
		k_1	k_2	k_3	k_4	k_5	k_6	k_7	k_8	k_9	
0	8.6956	3.9	10.7	0.9	9.9	10.1	6.0	-	-	-	Day 10 5.04
60	67.8816	10.7	10.8	4.8	10.5	10.0	2.5	10.1	10,0	9.9	Day 2 15,98
120	62.2039	15.3	10.9	4.7	9.2	10.3	4.2	10.2	10.0	10.0	Day 10 20.91
180	73.4293	19.9	10.7	5.2	8.1	10.4	5.4	10.2	10.0	10.0	Day 10 27.53
180/TiO₂	113.2106	17.0	10.9	4.5	9.1	10.2	4.6	10.2	10.0	10.0	Day 10 24.17
180/ZnCl₂	140.0404	15.1	10.9	3.7	9.8	10.2	3.1	10.2	10.0	10.0	Day 5 28.99
180/ZnO	49.6152	19.3	10.8	4.0	8.0	10.5	3.7	10.3	10.0	10.0	Day 10 26.12

In Model-3, the liquefaction of coal is therefore improved by three reversible reactions; In addition to Model-2, assuming that there are three reversible reactions between coal ↔ asphaltenes, asphaltenes ↔ oils and asphaltenes ↔ preasphaltenes, the experimental results given in Figure 4 and the modeling results are compatible. Compared to other models, Model-3 fits best with experimental data for UV power of 90, 120, 150, and 180W. Furthermore, the sum of the squared differences shown in Table 5 also proves that Model-3 has a better explanation for liquefaction of coal compared to the other two models. It also shows that the models fit better with experimental results at higher UV powers of 180 W compared to 90 W with lower UV powers. Thanks to these three reversible reactions, which are the only difference from Model-2, Model-3 fits much better with the experimental data. Thus, the main free radicals are formed from reactive coal, as mentioned above, and many competitive and simultaneous chemical reactions can occur during the liquefaction of reactive coals (Şimşek et al., 2017).

The reaction rate constants of Model-3 at four different UV powers, 90, 120, 150, and 180 W, were determined using multiple regression analysis and the results are presented in Table 5. The calculated rate constants for Model 4 at four different UV powers are given in Table 6 and the comparison of the liquefaction mechanism data obtained by modeling with the experimental data is given in Figure 5.

Comparison of the liquefaction mechanism obtained using model 5 with experimental data at different UV power is given in Figure 6 and the data obtained from Model 5 and the squares of the experimental data and the rate constants and oil formation percentages at different UV light powers are given in Table 7 respectively.
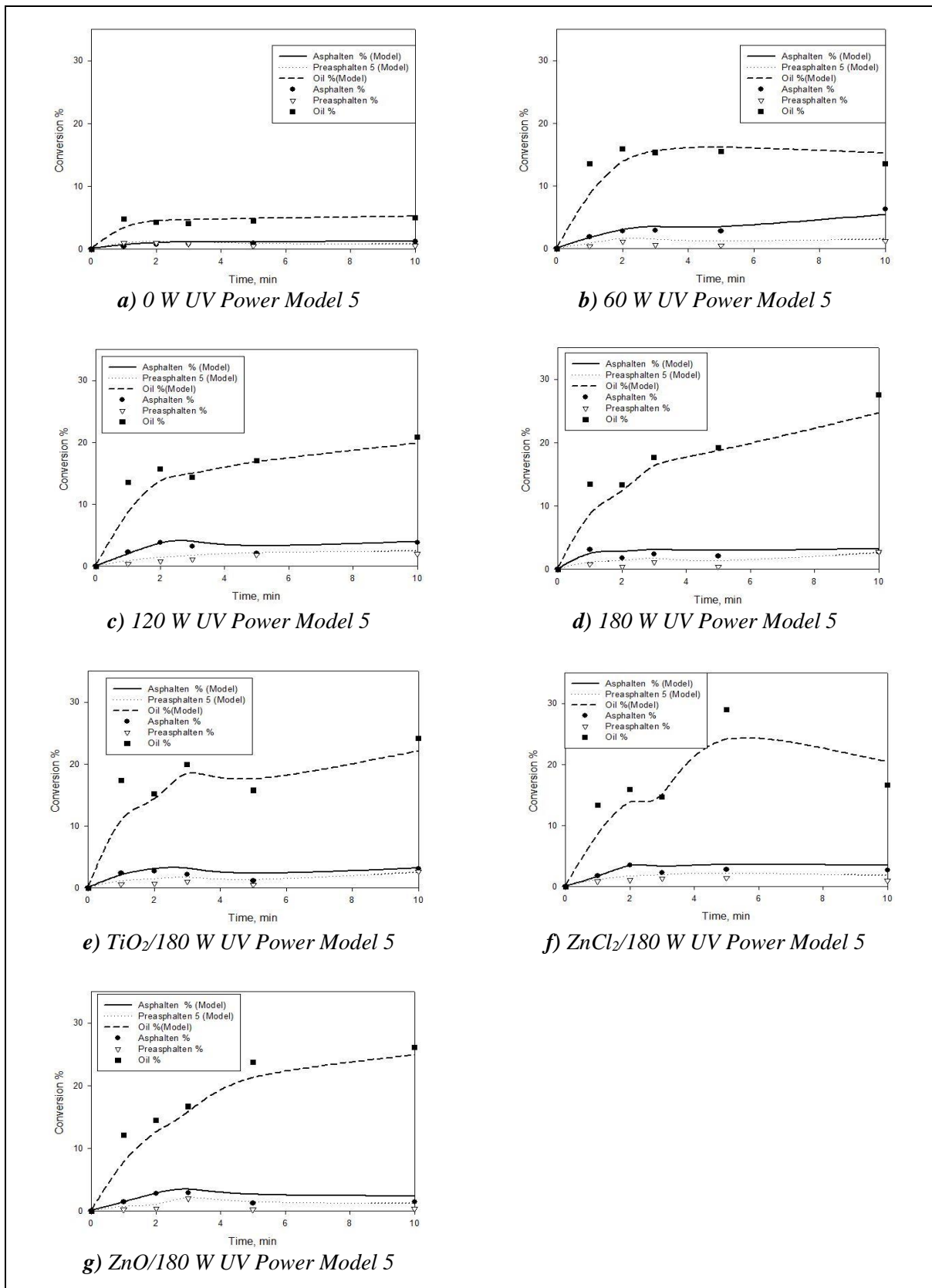
Figure 4. Comparison of the liquefaction mechanism obtained using Model 3
with experimental data at different UV powers
a) 0 W, b) 60 W, c) 120 W, d) 180 W e) TiO₂/180 W f) ZnCl₂/180 W g) ZnO/180 W

Figure 4. *Comparison of the liquefaction mechanism obtained using Model 3*
with experimental data at different UV powers
a) 0 W, b) 60 W, c) 120 W, d) 180 W e) TiO_2/180 W f) $ZnCl_2$/180 W g) ZnO/180 W

a) 0 W UV Power Model 4

b) 60 W UV Power Model 4

c) 120 W UV Power Model 4

d) 180 W UV Power Model 4

e) TiO₂/180 W UV Power Model 4

f) ZnCl₂/180 W UV Power Model 4

g) ZnO/180 W UV Power Model 4

Figure 5. *Comparison of the liquefaction mechanism obtained using Model 4*
with experimental data at different UV powers
a) 0 W, b) 60 W, c) 120 W, d) 180 W e) TiO₂/180 W f) ZnCl₂/180 W g) ZnO/180 W

Table 6. *The data obtained from Model 4 and the squares of the experimental data and the rate constants and the oil formation percentages at different UV light powers*

UV Power (W)	$\sum_i (y_{m_i} - y_{e_i})^2$	Rate constant (h^{-1}) x 10^3									oil conversion % experimental
		k_1	k_2	k_3	k_4	k_5	k_6	k_7	k_8	k_9	
0	8.3350	8.0	4.8	0.3	10.6	10.0	10.1	9.8	11.1	9.8	Day 10 5.04
60	65.0700	4.7	12.6	19.0	10.6	9.9	10.1	9.7	12.0	10.1	Day 2 15.98
120	61.9166	4.5	17.2	3.6	10.6	10.0	10.2	9.0	10.8	8.9	Day 10 20.91
180	75.5692	5.1	21.7	4.9	10.6	10.0	10.3	8.0	9.4	7.8	Day 10 27.53
180/TiO_2	112.5464	4.4	19.1	4.1	10.6	10.0	10.2	8.9	11.0	8.7	Day 10 24.17
180/$ZnCl_2$	137.4485	3.6	17.3	2.5	10.7	10.0	10.2	9.3	12.6	9.3	Day 5 28.99
180/ZnO	51.9861	3.9	21.1	3.2	10.6	10.0	10.3	7.7	9.5	7.6	Day 10 26.12

Table 7. *The data obtained from Model 5 and the squares of the experimental data and the rate constants and the oil formation percentages at different UV light powers*

UV Power (W)	$\sum_i (y_{m_i} - y_{e_i})^2$	Rate constant (h^{-1}) x 10^3									oil conversion % experimental
		k_1	k_2	k_3	k_4	k_5	k_6	k_7	k_8	k_9	
0	8.3925	10.0	10.7	2.5	10.1	10.1	9.8	4.6	11.1	9.8	Day 10 5.04
60	65.2008	5.0	10.8	2.1	10.0	10.1	9.7	12.4	12.0	10.1	Day 2 15.98
120	61.8398	4.8	10.9	3.7	10.3	10.2	9.0	17.0	10.8	8.9	Day 10 20.91
180	75.5094	5.4	10.7	4.9	10.5	10.4	8.0	21.5	9.4	7.8	Day 10 27.53
180/TiO_2	112.6105	4.7	10.9	4.1	10.3	10.2	8.9	18.9	11.0	8.7	Day 10 24.17
180/$ZnCl_2$	137.4365	3.9	10.9	2.6	10.3	10.2	9.3	17.1	12.6	9.4	Day 5 28.99
180/ZnO	51.9647	4.2	10.7	3.3	10.5	10.3	7.7	20.9	9.5	7.6	Day 10 26.12

Figure 6. *Comparison of the liquefaction mechanism obtained using Model 5
with experimental data at different UV powers
a) 0 W, b) 60 W, c) 120 W, d) 180 W e) TiO₂/180 W f) ZnCl₂/180 W g) ZnO/180 W*

The reaction rate from reactive charcoal to oils is four times more compared to other reaction rate constants shown in 3rd Model. The reaction rate constant for the liquefaction reaction from reactive coal to oils is about 10.0×10^{-3} h^{-1}, while the reaction rate constants for the other reactions in the model are about $2.5.0 \times 10^{-3}$ h^{-1}. Additionally, UV forces affect the reaction rate constants of Beypazarı coal liquefaction reaction are insignificantly. Model 4 and Model 5 liquefaction mechanism rate constants are very close to each other. Simultaneously, the square of the difference between the experimental data and the data obtained from the model, in other words, the compatibility of the experimental data with the experimental data is very close to each other and the data obtained from Model 3. When these results are evaluated together, it has been shown that models with reversible reactions are quite successful in explaining the liquefaction mechanism of Beypazarı coals. Therefore, Model 3, Model 4 and Model 5 include model mechanisms suitable for Beypazarı liquefaction process.

The general liquefaction steps of a reactive coal consist of four steps;

(i)   bond cleavage between structural species and then

(ii)   stabilization of free radicals by breaking bonds by hydrogen transfer, and then either

(iii)   formation of liquefied molecules of smaller molecular weight or

(iv)   repolymerization of free radicals due to hydrogen deficiency. The formation of high molecular weight of poly-aromatic species similar to Char can cause depolymerization.

The increase in oil yield during the liquefaction process can be attributed to the stabilization of free radicals by hydrogen transfer from hydrogen-rich hydrocarbons instead of hydrogen donor solvent (Şimşek et al., 2017). The presence of reversible reactions in the liquefaction model prove that the hydrogen donor solvent can not be able to transfer sufficient hydrogen to free radicals (Şimşek et al., 2020) This study shows that reversible reaction steps are the decisive steps in the liquefaction of Beypazarı lignite under UV power. Additionally, reversible models show the best agreement with experimental data regardless of reaction steps, coal types, and power sources such as UV (Şimşek et al., 2017; 2019). However, with the use of catalyst in the experimental data, an increase in the yield of the liquid product stands out. In particular, the use of $ZnCl_2$ led to a more effective yield in a shorter time. However, the data obtained from the experimental data and the model show the compatibility of the most compatible model with the use of catalyst and the studies conducted without UV power. In other words, in the experimental and modeling studies conducted with 0 Watt UV power in a catalyst-free environment, the harmony gives the best results between Model 3-4 and Model 5.

Experimental data show that oil yields increase with increasing UV use. The modeling work performed in Model 4, which includes reversible reactions in parallel with the experimental studies, draw attention as the model most compatible with the experimental data. It was also found that the liquefaction step from coal to oils had the highest reaction rate constant compared to the reactions given in other models proposed in Model-4. Also, the reaction rate constants are independent of the liquefaction power in the liquefaction process using UV as the liquefaction power source. Apart from this study, another study on the liquefaction of Beypazarı coals under UV power is the study of Şimşek et al. (2019). They showed that reversible steps play a major role in the liquefaction mechanism in his study. Additionally, the aforementioned study also showed that the Kalman filter is one of the useful methods to estimate the model parameter for liquefaction of coals using minimal experimental results (Şimşek, 1997). Şimşek et al. (2020) did not suggest any mechanism in the catalyst environment for Beypazarı coal based on experimental data with modeling of the mechanism. In this publication, in addition to the work of Şimşek (1997), it is focused on the liquefaction mechanism modeling of the experimental studies conducted in the catalyst environment. The efficiency of TiO_2, $ZnCl_2$, and ZnO catalysts under 180 Watt UV power, where the experimental data gave the best results, was examined both experimentally and model. While the experimental data revealed that the oil yields were much higher in the environments with ZnO catalysts, it was concluded that Model 4 gave the appropriate values in the presence of ZnO catalyst in the modeling studies.

Additionally, when the elemental analysis of the coal used in the experiments is considered, especially in terms of O content, it is striking that the sample is a very young lignite. Also, Both ash and maceral content of the coal used in the experiments show a diluting effect during the liquefaction process. Maseral density increases in the order of liptinite <vitrinite <inertinite. Due to the different vegetative tissues that make up the macerals, the molecular structures of the macerals are also different. The different properties and behavior of the macerals are the result of their different molecular structures. In the amount of combustible volatile matter and easily volatile fixed carbon, approximately 40% of the mass, carbon has the feature of formation change due to bond breaking easily according to the structural features. Due to the mentioned structural feature, the potential of obtaining liquid products is high thanks to the hydrogenation provided by tetralin in liquefaction for the sample of Beypazarı lignite.

4. CONCLUSION

Model 2, Model 3, Model 4 and Model 5, where parallel reactions form products, is more compatible with the experimental results of liquefaction using 5/1 tetralin/coal ratio from reactive charcoal than Model 1, which includes serial reactions. Although the experimental oil yields are low in the experimental studies based on the use of UV, when the modeling studies are compared with the experimental data, the most compatible data is seen to be quite compatible in the experiments conducted in the dark, especially in Model 4, without using the UV power. Notably, the conversion rate constants from asphaltene to oil, from asphaltene to preasphalten, and from preasphalten to oil in Model 4 in the dark environment are higher than the other formations. Model 3, Model 4 and Model 5 consist of reversible reaction steps in addition to parallel liquefaction steps. Here, it makes the liquefaction kinetics of Beypazarı coal much better understood. In the experiments conducted with the catalyst, 180 Watt UV power, which is the UV power with the highest efficiency, was used. However, there is not much difference in terms of oil yield between the use of catalyst and the studies conducted in a catalyst-free environment, and the closeness of the experimental data with the data obtained from the model was found to be more compatible with Model 4.

Although the applicability of UV power for coal liquefaction in mass production is very difficult due to the long reaction time, it is thought that this study can be a guide for the design of UV Lamp Photochemical Reactor in the presence of catalysts of pilot scale liquefaction processes. Additionally, this work can lead to the formation of higher quality (low molecular weight) liquid products in thermal coal liquefaction process supported by UV irradiation energy. Additionally, in future studies, it will be more meaningful to explain the reaction rate steps more clearly and to establish mechanisms that can interfere with the reaction in terms of the efficiency of the coal liquefaction process.

CONFLICTS OF INTEREST

The authors declare no conflict of interest.

REFERENCES

Allen, D. T., & Gavalas, G. R. (1984). Reactions of methylen and ether bridges. *Fuel*, *63*(5), 586-592. doi:10.1016/0016-2361(84)90150-9

Angelova, G., Kamenski, D., & Dimova, N. (1989). Kinetics of donor-solvent liquefaction of Bulgarian brown coal. *Fuel*, *68*(11), 1434-1438. doi:10.1016/0016-2361(89)90042-2

Ayappa, K. G., Davis, H. T., Davis, E. A., & Gordon, J. (1991). Analysis of microwave heating of materials with temperature-dependent properties. *AIChE J*, *37*(3), 313-322. doi:10.1002/aic.690370302

Ceylan, K., & Olcay, A. (1998). Kinetic rate models for dissolution of Turkish lignites in tetralin under nitrogen or hydrogen atmospheres. *Fuel Processing Technology*, *53*(3), 183-195. doi:10.1016/S0378-3820(97)00054-4

Cronauer, D. C., Shah, Y. T., & Ruberto, R. G. (1978). Kinetics of thermal liquefaction of Belle Ayr subbituminous coal. *Industrial & Engineering Chemistry Process Design and Development*, *17*(3), 281-288. doi:10.1021/i260067a013

Cronauer, D. C., Jewell, D. M., Shah, Y. T., & Modi, R. J. (1979). Mechanism and kinetics of selected hydrogen transfer reactions typical of coal liquefaction. *Industrial & Engineering Chemistry Fundamentals*, *18*(2), 153-162. doi:10.1021/i160070a011

Cunliffe, B. (Ed.). (2001). *The Oxford illustrated history of prehistoric Europe*. Oxford Illustrated History.

Doetschman, D. C., Ito, E., Ito, O., & Kameyama, H. (1992). Photochemical extraction from tetrahydrofuran slurries of representative coals. *Energy & Fuels*, *6*(5), 635-42. doi:10.1021/ef00035a015

Farcasiu, M., Mitchell, T. O., & Whitehurst, D. D. (1977). Asphaltols - Keys to Coal Liquefaction. *Chemtech*, *7*, 680-686.

Gao, D., Ye, C., Ren, X., & Zhang, Y. (2018). Life cycle analysis of direct and indirect coal liquefaction for vehicle power in China. *Fuel Processing Technology*, *169*, 42-49. doi:10.1016/j.fuproc.2017.09.007

Grewal, M. S., & Andrews, A. P. (2001). *Kalman Filtering: Theory and Practice Using MATLAB* (2nd ed.). John Wiley & Sons.

Han, K. W., Dixit, V. B., & Wen, C. Y. (1978). Analysis and scale-up consideration of bituminous coal liquefaction rate processes. *Industrial & Engineering Chemistry Process Design and Development*, *17*(1), 16-21. doi:10.1021/i260065a004

Hao, P., Bai, Z.-Q., Zhao, Z.-T., Yan, J.-C., Li, X. Guo, Z.-X., Xu, J.-L., Bai, J., & Li, W. (2017). Study on the preheating stage of low rank coals liquefaction: product distribution, chemical structural change of coal and hydrogen transfer. *Fuel Processing Technology*, *159*, 153-159. doi:10.1016/j.fuproc.2017.01.028

Hao, P., Bai, Z.-Q., Zhao, Z.-T., Ge, Z.-F., Hou, R.-R., Bai, J., Guo, Z.-X., Kong, L.-X., & Li, W. (2018). Role of hydrogen donor and non-donor binary solvents in product distribution and hydrogen consumption during direct coal liquefaction. *Fuel Processing Technology*, *173*, 75-80. doi:10.1016/j.fuproc.2018.01.012

Hsiang-Hui, K., & Stock, L. M. (1984). Aspects of the chemistry of donor solvent coal dissolution: Promotion of the bond cleavage reactions of diphenylalkanes and the related ethers and amines. *Fuel*, *63*(6), 810-815. doi:10.1016/0016-2361(84)90072-3

Huang, H., Wang, K., Wang, S., Klein, M. T., & Calkins, W. H. (1998). Studies of coal liquefaction at very short reaction times. 2. *Energy & Fuels*, *12*(1), 95-101. doi:10.1021/ef970073c

Kalman, R. E. (1960). A new approach to linear filtering and prediction problems. *J. Basic Eng.*, *82*(1), 35-45. doi:10.1115/1.3662552

Karacan, F. (2004). *Ultraviyole Işınların Katalizörlü Ortamda Kömür Sıvılaşmasına Etkisi*. PhD Thesis, Ankara University.

Kavuştu, H. (2012). *Kömürlerin Tetralinde UV Işınları ve Mikrodalga Enerji ile Sıvılaşma Mekanizmalarının Kesikli Zaman Modelleri Kullanılarak Belirlenmesi*. MSc Thesis, Ankara University.

Li, X., Hu, H., Zhu, S., Hu, S., Wu, B., & Meng, M. (2008). Kinetics of coal liquefaction during heating up and isothermal stages. *Fuel*, *87*(4-5), 508-513. doi:10.1016/j.fuel.2007.03.041

Li, W., Bai, Z.-Q., Bai, J., & Li, X. (2017). Transformation and roles of inherent mineral matter in direct coal liquefaction: a mini-review. *Fuel*, *197*, 209-216. doi:10.1016/j.fuel.2017.02.024

Liebenberg, B. J., & Potgieter, H. G. J. (1973). The uncatalysed hydrogenation of coal. *Fuel*, *52*(2), 130-133. doi:10.1016/0016-2361(73)90036-7

Liu, R., Li, Y., Wang, C., Xiao, N., He, L., Guo, H., Wan, P., Zhou, Y., & Qiu, J. (2018). Enhanced electrochemical performances of coal liquefaction residue derived hard carbon coated by graphene as anode materials for sodium-ion batteries. *Fuel Processing Technology*, *178*, 35-40. doi:10.1016/j.fuproc.2018.04.033

Mohan, G., & Silla, H. (1981). Kinetics of donor-solvent liquefaction of bituminous coals in nonisothermal experiments. *Industrial & Engineering Chemistry Process Design and Development*, *20*(2), 349-358. doi:10.1021/i200013a026

Shah, Y. T., Cronauer, D. C., McIlvried, H. G., & Paraskos, J. A. (1978). Kinetics of catalytic liquefaction of Big Horn coal in a segmented bed reactor. *Industrial & Engineering Chemistry Process Design and Development*, *17*(3), 288-301. doi:10.1021/i260067a014

Shalabi, M. A., Baldwin, R. M., Bain, R. L., Gary, J. H., & Golden, J. O. (1978). Kinetics of coal liquefaction. *Coal Processing Technology*, *4*, 82-86.

Shalabi, M. A., Baldwin, R. M., Bain, R. L., Gary, J. H., & Golden, J. O. (1979). Noncatalytic coal liquefaction in a donor solvent. Rate of formation of oil, asphaltenes, and preasphaltenes. *Industrial & Engineering Chemistry Process Design and Development*, *18*(3), 474-479. doi:10.1021/i260071a021

Shui, H., Chen, Z., Wang, Z., & Zhang, D. (2010). Kinetics of Shenhua coal liquefaction catalyzed by SO_4^{2-}/ZrO_2 solid acid. *Fuel*, *89*(1), 67-72. doi:10.1016/j.fuel.2009.02.019

Snape, C. E. (1987). Characterisation of organic coal structure for liquefaction. *Fuel Processing Technology*, *15*, 257-279. doi:10.1016/0378-3820(87)90050-6

Söğüt, F. (1997). *UV ışınları ile linyitlerin desülfürizasyonu*. PhD Thesis, Ankara University.

Söğüt, F., & Olcay, A. (1998). Dissolution of lignites in tetralin at ambient temperature: effects of ultraviolet irradiation. *Fuel Processing Technology*, *55*(2), 107-115. doi:10.1016/S0378-3820(98)00045-9

Speight, J. G. (2008). *Synthetic fuels handbook: properties, process and performance*. The McGraw-Hill Companies, Inc.

Şimşek, E. H. (1997). *Türk kömürlerinin mikrodalga enerji etkisiyle tetralindeki hidrojenasyonu*. PhD Thesis, Ankara University.

Şimşek, E. H., Karaduman, A., & Olcay, A. (2001). Investigation of dissolution mechanism of six Turkish coals in tetralin with microwave energy. *Fuel*, *80*(15), 2181-2188. doi:10.1016/S0016-2361(01)00102-8

Şimşek, E. H., Güleç, F., & Kavuştu, H. (2017). Application of Kalman filter to determination of coal liquefaction mechanisms using discrete time models. *Fuel*, *207*, 814-820. doi:10.1016/j.fuel.2017.06.004

Şimşek, E. H., Güleç, F., Kavuştu, H., & Karaduman, A. (2019). Determination of liquefaction mechanisms of Zonguldak, Soma and Beypazarı coals using discrete time models. *Journal of the Faculty of Engineering and Architecture of Gazi University*, *34*(1), 79-88. doi:10.17341/gazimmfd.416464

Şimşek, E. H., Güleç, F., & Akçadağ, F. S. (2020). Understanding the liquefaction mechanism of Beypazarı lignite in tetralin with ultraviolet irradiation using discrete time models. *Fuel Processing Technology*, *198*, 106227. doi:10.1016/j.fuproc.2019.106227

Wang, Z., Shui, H., Zhu, Y., & Gao, J. (2009). Catalysis of SO_4^{2-}/ZrO_2 solid acid for the liquefaction of coal. *Fuel* 88, 885-889. doi:10.1016/j.fuel.2008.10.040

Wei, L., Jian, Z., Chunzhi, W., & Hui, X. (2013). Kalman filter Localization algorithm based on SDS-TWR ranging. *TELKOMNIKA Indonesian Journal of Electrical Engineering, 11*(3), 1436-48. doi:10.11591/telkomnika.v11i3.2225

Welch, G., & Bishop, G. (2006). *An introduction to the Kalman filter* (Technical Report: TR 95-041). University of North Carolina at Chapel Hill.

Yürüm, Y., & Yiğinsu, I. (1982). Depolymerization of Turkish lignites: 3. Effect of ultraviolet radiation. *Fuel*, *61*(11), 1138-1140. doi:10.1016/0016-2361(82)90200-9